SCIENCE CHINA
Information Sciences

• LETTER •

September 2026, Vol. 69, Iss. 9, 199301:1–199301:2
https://doi.org/10.1007/s11432-026-5031-5

First experimental validation of repeat-pass GEO D-InSAR deformation monitoring using LuTan-4 satellite

Yuanhao LI[1], Cheng HU[1*], Qingjun ZHANG[2], Zhiyang CHEN[1], Xingzhe ZHAO[1], Yuxiao WANG[1], Xinwei ZHAO[3] & Yong ZENG[3]

[1]*School of Information and Electronics, Beijing Institute of Technology, Beijing 100081, China*
[2]*China Academy of Space Technology, Beijing 100094, China*
[3]*China Centre for Resources Satellite Data and Application, Beijing 100094, China*

Received 5 June 2026/Revised 26 June 2026/Accepted 2 July 2026/Published online 13 August 2026

Citation Li Y H, Hu C, Zhang Q J, et al. First experimental validation of repeat-pass GEO D-InSAR deformation monitoring using LuTan-4 satellite. Sci China Inf Sci, 2026, 69(9): 199301, https://doi.org/10.1007/s11432-026-5031-5

The geosynchronous synthetic aperture radar (GEO SAR), operating at an altitude of approximately 36000 km, provides a large swath (hundreds to thousands of kilometers) and a high temporal resolution (hours to one day) [1], supporting wide-area geohazard monitoring and rapid disaster response.

China's LuTan-4, the first GEO SAR satellite launched in August 2023, features an L-band sensor achieving swaths of >500 km (<20 m resolution) in stripmap and >3000 km (<50 m resolution) in scanSAR modes [2]. Although not a dedicated interferometric system like SuperView Neo-2 [3] or LuTan-1 [1], its relatively low-frequency orbital control strategy combined with a proper repeat-pass interferometric data selection method can yield the repeat-pass interferometric perpendicular baselines within the critical baselines, which brings GEO SAR the capability of differential interferometric SAR (D-InSAR) applications.

Previous studies have investigated GEO D-InSAR concepts, processing methods, and performance mainly through theoretical analyses [4]. In this letter, we experimentally validate the GEO D-InSAR deformation monitoring capability for the first time based on real LuTan-4 satellite data. A processing framework is proposed to address problems of non-parallel repeat-pass tracks, inaccurate orbital ephemeris, and spatially variant atmospheric phases within a large swath in GEO D-InSAR. Real repeat-pass LuTan-4 SAR data spanning a nearly 120 km × 80 km sub-scene with a one-day revisit were used to validate the processing framework and demonstrate its D-InSAR deformation monitoring capability.

Method and processing framework. The GEO D-InSAR processing framework is shown in Figure 1(a). The framework takes the master and slave images, external digital elevation model (DEM), and external atmospheric data as inputs. The detailed processing flow is introduced as follows.

Step 1: Optimal repeat-pass data selection. Due to the Earth rotation effect, the repeat-pass tracks suffer non-parallel effects, and the antenna beam is generally squinted, which can introduce severe Doppler decorrelation and rotational decorrelation in the interferogram [4]. To address this issue, we adopt an optimal repeat-pass GEO D-InSAR data selection method, which is to select the interferometric pair with a maximum geometric coherence. The geometric coherence model can be expressed as [5]

$$\gamma \approx \frac{\sqrt{\boldsymbol{u}^{\mathrm{T}}\cdot\boldsymbol{e}_{\mathrm{M}}}\sqrt{\boldsymbol{u}^{\mathrm{T}}\cdot\boldsymbol{e}_{\mathrm{S}}}}{\boldsymbol{u}^{\mathrm{T}}\cdot\boldsymbol{e}_2}\cdot \left[1-\frac{|\mathrm{c}\cdot\Delta\boldsymbol{u}^{\mathrm{T}}\cdot\boldsymbol{e}_2|}{|\lambda B\cdot\boldsymbol{u}_{\mathrm{g}}^{\mathrm{T}}\cdot\boldsymbol{e}_2|}\right]\cdot\left[1-\frac{|R\cdot\Delta\boldsymbol{u}^{\mathrm{T}}\cdot\boldsymbol{e}_1|}{|\boldsymbol{L}^{\mathrm{T}}\cdot\boldsymbol{e}_1|}\right], \tag{1}$$

where $\boldsymbol{e}_{\mathrm{M}}$ and $\boldsymbol{e}_{\mathrm{S}}$ denote the Doppler directions of the master and slave observations, respectively; $\boldsymbol{e}_1$ and $\boldsymbol{e}_2$ represent the iso-Doppler direction of the master and slave tracks; $\boldsymbol{u}$ is the equivalent synthetic aperture vector of the interferometric pair; λ is the radar wavelength; c is the speed of light; $\Delta\boldsymbol{u}$ denotes the line-of-sight (LOS) variation between the master and slave observations; B is the signal bandwidth; $\boldsymbol{u}_{\mathrm{g}}$ is the ground-range direction; R is the slant range, and $\boldsymbol{L}$ denotes the ground projection of the synthetic aperture vector of the interferometric pair.

Step 2: Refocusing and coregistration. Due to the long integration time of GEO SAR, SAR image defocusing and interferometric coherence deterioration occur. To address this issue, Phase Gradient Autofocus is applied to improve the image quality [4]. Then, the interferometric SAR pairs are coregistered, and the corresponding interferogram is generated.

Step 3: Baseline estimation and reference phase removal. Due to the inaccurate ephemeris, the theoretical repeat-pass baseline is not accurate. To address this issue, a baseline estimation method based on Chirp-Z Transform (CZT) is applied [6], which utilizes the linear interferometric phase, primarily induced by the flat Earth, to estimate the baseline (mainly perpendicular and parallel components) as follows:

$$\boldsymbol{b} = \arg\min_{\boldsymbol{b}}\left(\varphi_{\mathrm{linear}} - \frac{4\pi}{\lambda}\langle\hat{\boldsymbol{l}},\boldsymbol{b}\rangle\right)^2, \tag{2}$$

where $\varphi_{\mathrm{linear}}$ is the estimated linear phase component, and $\hat{\boldsymbol{l}}$ is the LOS unit vector. Using the estimated baseline and the external DEM, the reference phase is generated and subsequently removed.

* Corresponding author (email: cchchb@163.com)

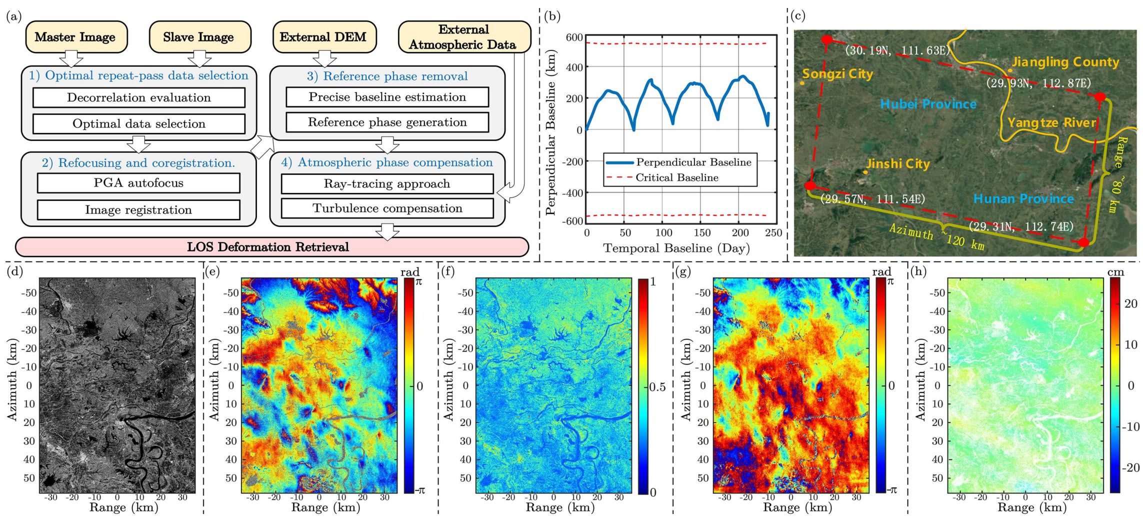

Figure 1 (Color online) Illustration of the GEO D-InSAR processing framework and results. (a) Proposed GEO D-InSAR processing framework; (b) long-term perpendicular baselines of LuTan-4 under optimal interferometric data selection [5]; (c) optical image of the observed area; (d) amplitude image of the GEO SAR; (e) interferogram after flat Earth phase removal; (f) coherence map; (g) compensated atmospheric phase, including ionospheric and tropospheric phases; (h) retrieved deformation after 10×10 multiple looks over regions with coherence higher than 0.4.

Step 4: Atmospheric phase compensation. GEO D-InSAR interferograms are easily contaminated by spatially variant atmospheric phases due to their large swaths, including ionospheric and tropospheric phases. The large-scale tropospheric and ionospheric phases are compensated using numerical weather prediction (NWP) data and total electron content (TEC) data, respectively. Both phases are calculated and compensated along the LOS direction using a ray-tracing approach. The small-scale atmospheric phases from turbulence typically follow a power-law spatial spectrum. To mitigate this effect, high-coherence pixels are first selected, and the power spectral density (PSD) of the residual phase is iteratively fitted to a PSD model. Based on the model, a Wiener filter is applied to remove the turbulence phase.

Finally, the differential phase is converted to deformation by $d = \varphi \cdot \lambda/(4\pi)$, where φ represents the D-InSAR phase, and d denotes the deformation along the LOS direction.

Results and discussion. The real repeat-pass LuTan-4 data are used to demonstrate their capability for D-InSAR processing. Firstly, from Figure 1(b), it can be seen that LuTan-4's perpendicular baselines are within the critical baselines, provided a low-frequency orbital control strategy and an optimal repeat-pass interferometric data selection method. After data selection, the repeat-pass LuTan-4 data acquired on August 10 and August 11, 2025 (perpendicular baseline = 12.49 km), with high geometric correlation, are used for D-InSAR processing, which have a synthetic aperture time of 30 min and a spatial resolution of 7.5 m (azimuth) $\times$ 12.6 m (range). As shown in Figure 1(c), the imaging area covers the main stream region of the Yangtze River at the border region between Hunan and Hubei provinces, with a swath of about 120 km $\times$ 80 km. The amplitude of the corresponding master image is presented in Figure 1(d), where the Yangtze River, the urban areas, and surrounding mountainous terrain are clearly visible, demonstrating the effect of the autofocus method.

The interferometric phase, shown in Figure 1(e), exhibits clear and continuous fringes corresponding to terrain variations and atmospheric components. Meanwhile, the coherence map in Figure 1(f) shows that the correlation coefficient is higher than 0.5 over most regions, indicating a good quality of the interferogram.

The compensated atmospheric phase, including ionospheric and tropospheric phases, is shown in Figure 1(g). After atmospheric phase compensation, the final deformation retrieval result is obtained, as shown in Figure 1(h) (processed with 10×10 multiple looks, retaining points with coherence higher than 0.4). Since the repeat-pass interval is only one day, we assume there is no significant ground deformation during this period. The retrieved deformation remains close to zero across the entire scene, indicating good deformation retrieval performance. Taking zero deformation as a reference, a root-mean-square error (RMSE) of 1.06 cm through the deformation map is obtained. This primarily derives from the residual phase noise and atmospheric phases. These results demonstrate the feasibility of the proposed interferometric processing framework as well as the capability of deformation monitoring using LuTan-4.

Conclusion. In this letter, we present the first experimental validation of repeat-pass GEO D-InSAR deformation monitoring using LuTan-4 satellite data. Real one-day repeat-pass SAR observations acquired over the Hunan-Hubei border area were processed using the proposed interferometric framework, achieving a deformation retrieval accuracy of 1.06 cm (RMSE). These results confirm the effectiveness of the processing strategy and provide the first real-data evidence that LuTan-4 is capable of monitoring deformation at the centimeter level with a one-day revisit. Further work will extend the assessment to additional scenarios to more comprehensively evaluate its D-InSAR performance.

Acknowledgements This work was supported by National Natural Science Foundation of China (Grant No. W2511068).

References

1 Hu C, Li Y H, Chen Z Y, et al. Distributed spaceborne SAR: a review of systems, applications, and the road ahead. IEEE Geosci Remote Sens Mag, 2025, 13: 329–361
2 Zhang Q J, Ni C, Dai C, et al. System design and key technologies of No.4 land exploration satellite 01. Chin Space Sci Techn, 2025, 45: 1–11
3 Chen J L, Liu Y Y, Li Y H, et al. Pioneering demonstration of large-baseline bistatic SAR in China: first experiment with SuperView Neo-2 satellites. Sci China Inf Sci, 2025, 68: 217301
4 Long T, Hu C, Ding Z G, et al. Geosynchronous SAR: System and Signal Processing. Singapore: Springer, 2018
5 Chen Z Y, Li Y H, Li C, et al. Analysis of general geometric decorrelation in interferometric SAR. IEEE Geosci Remote Sens Lett, 2022, 19: 1–5
6 Chen Z Y, Li Y H, Hu C, et al. Repeat-pass space-surface bistatic SAR tomography: accurate imaging and first experiment. Sci China Inf Sci, 2024, 67: 192304